Revue des Energies Renouvelables Vol. 14 N°1 (2011) 131 – 144
DOI: https://doi.org/10.54966/jreen.v14i1.247

Conception of robust neural networks to improve hybrid control of an induction motor

Malika Laribi[1*], Linda Barazane[2†], Chérif Larbès[1] and Ali Malek[3‡]

[1] Laboratoire des Dispositifs de Communication et de Conversion Photovoltaïque, 'LDCCP'
Département d'Electronique, Ecole Nationale Polytechnique
B.P. 182, Avenue Hassen Badi, El Harrach, Alger, Algérie
[2] Faculté d'Electronique et d'Informatique, Université des Sciences et de la Technologie Houari Boumediene, 'USTHB', B.P. 32, El Alia, Bab Ezzouar, Alger, Algérie
[3] Division Energie Solaire Photovoltaïque
Centre de Développement des Energies Renouvelables, 'CDER'
B.P. 62, Route de l'Observatoire, Bouzaréah, Alger, Algérie

(reçu le 5 Septembre 2010 - accepté le 26 Mars 2011)

Abstract - *Neural networks and fuzzy controllers are considered as the most efficient approximators of different functions and have also proved their capability of controlling nonlinear dynamical systems. So, in this paper, the authors introduce a novel technique of control called 'hybrid control' which is Based on Feedback Linearization and Field Oriented Control of an Induction Motor, in order to replace the sliding mode controllers (speed and flux ones). In fact, the objectives required by the introduction of neural networks, 'RANNCs' is to perform the control which is shown by simulation results.*

Résumé – *Les réseaux de neurones et de contrôleurs flous sont considérés comme les plus efficaces approximateurs des différentes fonctions et ont également montré leur capacité de contrôler des systèmes non linéaires. Ainsi, dans cet article, les auteurs ont introduit une nouvelle technique de contrôle appelée 'contrôle hybride', basée sur le feedback de la linéarisation et sur la thématique axée sur le contrôle d'un moteur à induction, afin de remplacer les contrôleurs de mode de glissement (vitesse et flux). En fait, les objectifs requis par l'introduction de réseaux de neurones (RANNCs) consistent à effectuer le contrôle, qui est démontré par les résultats de simulation.*

Key words: Induction motor - Field-oriented control - Sliding mode controller - Robust artificial neural networks controller - Leverberg-Marquart algorithm.

1. INTRODUCTION

Artificial neural networks, 'ANNs' try to mimic the nerves system in a mammalian brain into a mathematical model. Therefore, ANNs have some desirable characteristics and capabilities similar to the brain system, such a parallel processing, learning, non-linear mapping, and generalization [1, 2].

Earlier works on the mapping properties of these architectures have shown that neural networks are universal approximators. Various architectures of neural systems are studied in the literature such as: Feed forward neural networks, Gaussian radial basis function neural networks and dynamical neural networks constitute typical structurally different approaches which have successfully been applied to problems extending from

* laribimpg@yahoo.fr , larbes_cher@yahoo.fr
† lbarazane@yahoo.fr
‡ amalek@cder.dz

control applications to electrical control process and identification of motors parameters [3, 4].

On the other hand, the control of the induction motor has attracted much attention in the last two decades. One of the most significant developments in this area has been the field-oriented control, 'FOC', where partial feedback linearization, together with a proportional integral, 'PI' controller is used to regulate the motor state [4, 5]. This technique is very useful, except that it is very sensitive to parameter variations [5].

To ensure good performance of the induction motor and the robustness of the feedback controller against parameter variations, unknown disturbances, initial conditions mismatch and load variations, different variables structures controllers were proposed [4][6, 7]. This type of control method consists of designing a sliding surface so that the plant has a desired system response. By proper design of the sliding surface, VSC can attain the conventional goals of control such as stabilization, tracking and regulation.

In this contribution, a control scheme based on the combination of feedback linearization and field-oriented controls with sliding mode control to achieve the goal of speed regulation is proposed. This technique consists of a decoupling method and sliding mode control.

Furthermore, and in order to reduce the chattering phenomenon, a new smooth piecewise function with a threshold is added in the control scheme.

A simulation study was carried out and the results revealed some very interesting features concerning the decoupling between the speed and rotor flux but the reduction of chattering is not sufficient which represents an inconvenient for the actuators, so, in order to perform the control and give a significant reduction in chattering, robust artificial neural networks, 'RANNCs' are investigated.

Such a control scheme could be associated to a photovoltaic system to ensure good performances in pumping water applications due to the robustness, the tracking of the functioning imposed reference etc....

2. FEEDBACK LINEARIZATION CONTROL (FLC)

The equations of the current-fed-model of the induction motor in the synchronous reference frame ($d^e - q^e$), with (i_{ds}, i_{qs}, ω_{ds}) as the command variables and (ϕ_{dr}, ϕ_{qr}, Ω) as the state variables are given by [4]:

$$\dot{x} = f(x) + g(x) \times u \tag{1}$$

where,

$$x = (x_1, x_2, x_3)^t = (\phi_{dr}, \phi_{qr}, \Omega)^t,\ u = (u_1, u_2, u_3)^t = (i_{ds}, i_{qs}, \omega_{sl})^t$$

$$f(x) = \begin{bmatrix} f_1(x) \\ f_2(x) \\ f_3(x) \end{bmatrix} = \begin{bmatrix} \dfrac{-x_1}{T_r} - p \times x_2 \times x_3 \\ \dfrac{-x_2}{T_r} - p \times x_1 \times x_3 \\ -\dfrac{T_L}{J} \end{bmatrix} \tag{2}$$

$$g(x)\times\left[g_1(x)\quad g_2(x)\quad g_3(x)\right]=\begin{bmatrix}\dfrac{L_m}{T_r} & 0 & p\times x_2\\ 0 & \dfrac{L_m}{T_r} & p\times x_1\\ \dfrac{-pL_m}{JL_r}\times x_2 & \dfrac{pL_m}{JL_r}\times x_1 & 0\end{bmatrix} \tag{3}$$

In order to attain the objectives of non-linear control, which consist in the control of the flux (ϕ_{dr} , ϕ_{qr} , Ω) it is advisable to choose the following three outputs variables:

$$\begin{aligned}\phi_1(x) &= \phi_{dr}\\ \phi_2(x) &= \phi_{qr}\\ \phi_3(x) &= \Omega\end{aligned} \tag{4}$$

The calculation of the relative degree r_i for each previous output $\phi_i(x)$ is equal to 1 respectively leading to:

$$\sum_{i=1}^{3} r_i = n = 3 \tag{5}$$

where: n is the system's order.

According to the new state variable, an exact linearization is obtained with:

$$\begin{aligned}z_1 &= \phi_1(x) = x_1\\ z_2 &= \phi_2(x) = x_2\\ z_3 &= \phi_3(x) = x_3\end{aligned} \tag{6}$$

The dynamic of the system is described by:

$$\begin{pmatrix}\dot{z}_1\\ \dot{z}_2\\ \dot{z}_3\end{pmatrix}=\begin{pmatrix}L_f h_1(x)\\ L_f h_2(x)\\ L_f h_3(x)\end{pmatrix}+D(x)\times\begin{pmatrix}u_1\\ u_2\\ u_3\end{pmatrix} \tag{7}$$

where the matrix $D(x)$ is given by

$$D(x)=\begin{pmatrix}L_{g1}h_1(x) & L_{g2}h_1(x) & L_{g3}h_1(x)\\ L_{g1}h_2(x) & L_{g2}h_2(x) & L_{g2}h_2(x)\\ L_{g1}h_3(x) & L_{g2}h_3(x) & L_{g3}h_3(x)\end{pmatrix} \tag{8}$$

and

$$L_{g1}h_1(x)=\frac{L_m}{T_r}\ ;\ L_{g2}h_1(x)=0;\ L_{g3}h_1(x)=-p\times x_1$$

$$L_{g1}h_2(x)=0\ ;\ L_{g2}h_2(x)=\frac{L_m}{T_r};\ L_{g3}h_2(x)=-p\times x_1$$

$$L_{g1}h_3(x)=-\frac{p\times L_m}{J\times L_r}x_2\ ;\ L_{g2}h_3(x)=\frac{p\times L_m}{J\times L_r}x_1;\ L_{g3}h_3(x)=0$$

$$\text{so,} \quad \det\left(D\left(x\right)\right) = \det\left(D\left(z\right)\right) = \frac{2L_m}{T_r} \times \frac{p \times L_m}{J \times L_r} \times \Phi_r^2 \tag{9}$$

It can be seen that $\det\left(D\left(z\right)\right) \neq 0$, since the flux $\Phi_r \neq 0$. In this case, the linearizing feedback is defined as follows:

$$\begin{pmatrix} u_1 \\ u_2 \\ u_3 \end{pmatrix} = \frac{1}{\det(D(z))} \times \begin{pmatrix} \frac{pL_m}{JL_r} z_1^2 & \frac{pL_m}{JL_r} z_1 z_2 & \frac{-L_m}{L_r} z_2 \\ \frac{pL_m}{JL_r} z_1 z_2 & \frac{pL_m}{JL_r} z_2^2 & \frac{L_m}{L_r} z_1 \\ \frac{L_m L_m}{L_r T_r} z_2 & \frac{-L_m L_m}{L_r T_r} z_1 & \left(\frac{L_m}{T_r}\right)^2 \end{pmatrix} \times \begin{pmatrix} \nu_1 + \frac{1}{T_r} z_1 \\ \nu_2 + \frac{1}{T_r} z_2 \\ \nu_3 + \frac{T_L}{J} \end{pmatrix} \tag{10}$$

The resulting system is described by the following equations

$$\begin{aligned} \dot{z}_1 &= \nu_1 \\ \dot{z}_2 &= \nu_2 \\ \dot{z}_3 &= \nu_3 \end{aligned} \tag{11}$$

The resulting diagram of the control system applied to an induction motor (with feedback linearization) is depicted in figure 1.

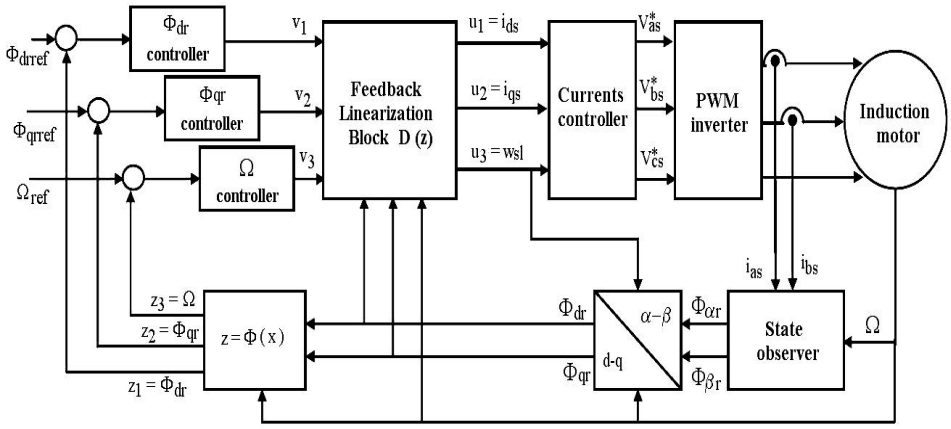

Fig. 1: Block diagram of the feedback linearization control

3. ASSOCIATION OF THE FEEDBACK LINEARIZATION AND THE FIELD ORIENTED CONTROL TECHNIQUES

In the case of a rotor-flux orientation, the regulator imposes the orientation of the rotor flux (Φ_r) with respect to the d^e axis, so, $\Phi_r = \Phi_{dr}$ and $\Phi_{qr} = 0$. Substituting these relations in (7) yields to:

$$\begin{pmatrix} \dot{z}_1 \\ \dot{z}_2 \end{pmatrix} = \begin{pmatrix} \frac{-1}{T_r} z_1 \\ \frac{-T_L}{J} \end{pmatrix} + \begin{bmatrix} \frac{L_m}{T_r} & 0 \\ 0 & \frac{pL_m}{JL_r} z_1 \end{bmatrix} \times \begin{pmatrix} u_1 \\ u_3 \end{pmatrix} \tag{12a}$$

$$\begin{pmatrix} \dot{z}_1 \\ \dot{z}_2 \end{pmatrix} = \begin{pmatrix} \frac{-1}{T_r} z_1 \\ \frac{-T_L}{J} \end{pmatrix} + D^*(z) \times \begin{pmatrix} u_1 \\ u_3 \end{pmatrix} \tag{12b}$$

In this case, the linearizing feedback is defined as:

$$\begin{pmatrix} u_1 \\ u_3 \end{pmatrix} = D^*(z)^{-1} \times \left\{ \begin{pmatrix} -L_f h_1 \\ -L_f h_2(x) \end{pmatrix} + \begin{pmatrix} \nu_1 \\ \nu_3 \end{pmatrix} \right\} \tag{13}$$

The resulting system is described by the following equations:

$$\begin{aligned} \dot{z}_1 &= \nu_1 \\ \dot{z}_3 &= \nu_3 \end{aligned} \tag{14}$$

4. INTRODUCTION OF THE SLIDING MODE CONTROL (SMC)

The basic principle of sliding mode control consists in moving the state trajectory of the system toward a predetermined surface called sliding surface $S(\bullet)$ and in maintaining it around this latter with an appropriate control law U which is of the form [4]:

$$U = U_{eq} + U_n \tag{15}$$

with,

$$U_n = -G(S(\bullet)) \times \mathrm{sgn}(S(\bullet))$$

and, U_{eq} : the equivalent control.

In a conventional SMC the reachability control generates a high control activity as it depends on the magnitude $M(\bullet)$ since it was first taken as constant, a relay function. This provoke a chattering phenomenon which is undesirable and its was a focus of many research works [4][6, 7].

In the present work the following function, which gives higher performances as it uses an exponential function for smoothing is proposed [4].

$$G(S) = \begin{cases} K - (K-k) \times \exp\left(\frac{|S(\bullet)| - \sigma}{\sigma} \right) -; & |S(\bullet)| > \varepsilon \\ \frac{k}{\varepsilon} -; & |S(\bullet)| \le \varepsilon \end{cases} \tag{16}$$

The constant K is linked to the speed of convergence towards the sliding surface of the process.

k is the minimal value of $M(S)$ which guarantees the robustness of the control.

In this paper, the resulting block diagram of the proposed controller using variable structure regulators is given in figure 2.

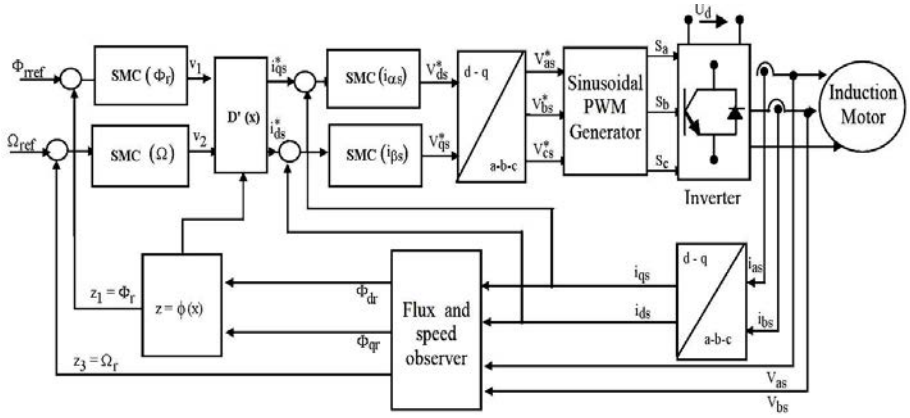

Fig. 2: Block diagram of the cascade sliding mode control of induction motor

4.1 Design of the switching surfaces

In this work, four sliding surfaces are considered:

$$\begin{aligned} S_1(z_1) &= e_1(z_1) = \Phi_{rref} - \Phi_r \\ S_2(z_3) &= e_2(z_3) = \Omega_{ref} - \Omega \\ S_3(u_1) &= e_3(u_1) = i_{ds}^* - i_{ds} \\ S_4(u_2) &= e_4(u_2) = i_{qs}^* - i_{qs} \end{aligned} \tag{17}$$

4.2 Development of the control laws

By using equation system (12), the two regulators' control laws, for the flux and the speed, of the external loop are given as follows:

4.2.1 For the flux regulator

$$S(\Phi_r) \times \dot{S}(\Phi_r) < 0 \quad \Rightarrow \quad i_{ds} = i_{dseq} + i_{dsn} \tag{18}$$

with

$$i_{dseq} = \frac{1}{L_m} \times \left(T_r \times \dot{\Phi}_{rref} + \Phi_r \right) \tag{18a}$$

$$i_{dsn} = -\left(K_1 - (K_1 - k_1) \times \exp\left(\frac{|S_1(z_1) - \varepsilon_1|}{\sigma} \right) \right) \times \operatorname{sgn}(S_1(z_1)) \tag{18b}$$

and, $S_1(z_1) > \varepsilon_1$

4.2.2 For the speed regulator

$$S(i_{qs}) \times \dot{S}(i_{qs}) < 0 \quad \Rightarrow \quad i_{qs} = i_{qseq} + i_{qsn} \tag{19}$$

with

$$i_{qseq} = \frac{L_r}{p \times L_m} \times \left(\frac{J \times \dot{\Omega}_{rref} + T_L}{\Phi_r} \right) \quad (19a)$$

$$i_{qsn} = -\left(K_2 - (K_2 - k_2) \times \exp\left(\frac{|S_2(z_3) - \varepsilon_2|}{\sigma} \right) \right) \times \mathrm{sgn}(S_2(z_3)) \quad (19b)$$

and, $S_2(z_3) > \varepsilon_2$

with: Φ_{rref} and Ω_{ref} the reference variables of the flux and the speed, respectively. $S_1(z_1)$ and $S_2(z_3)$ are related to the outer loop, whereas $S_3(u_1)$ and $S_4(u_3)$ are related to the inner loop.

4.2.3 For the control variable i_{ds}

$$S(i_{ds}) \times \dot{S}(i_{ds}) < 0 \quad \Rightarrow \quad V_{ds} = V_{dseq} + V_{dsn} \quad (20)$$

with

$$V_{dseq} = \sigma L_s \frac{d}{dt} i_{ds} + R_s i_{ds} - \sigma L_s \omega_r i_{qs} - \frac{L_m}{T_r} \omega_r \times \Phi_r \quad (20a)$$

$$V_{dsn} = -\left(K_3 - (K_3 - k_3) \times \exp\left(\frac{|S_3(z_1) - \varepsilon_3|}{\sigma} \right) \right) \times \mathrm{sgn}(S_3(u_1)) \quad (20b)$$

and, $S_3(u_1) > \varepsilon_3$

4.2.3 For the control variable i_{qs}

$$S(i_{qs}) \times \dot{S}(i_{qs}) < 0 \quad \Rightarrow \quad V_{qs} = V_{qseq} + V_{qsn} \quad (21)$$

with

$$V_{qseq} = \sigma L_s \frac{d}{dt} i_{qs} + R_s i_{qs} + \sigma L_s \omega_s i_{ds} + \frac{L_m}{T_r} \omega_r \times \Phi_r \quad (21a)$$

$$V_{qsn} = -\left(K_4 - (K_4 - k_4) \times \exp\left(\frac{|S_4(u_3) - \varepsilon_4|}{\sigma} \right) \right) \times \mathrm{sgn}(S_4(u_3)) \quad (21b)$$

and, $S_4(u_3) > \varepsilon_4$

To satisfy the stability condition of the system, the following gains (K_1, K_2, K_3, K_4) should be taken positive and with chosen appropriate values to obtain high performances.

5. TESTS AND SIMULATION

In order to verify the effectiveness of the proposed approach, some simulation studies were carried out. The squirrel-cage induction motor used in the simulation is a 2 poles machine with a 1.5 kW rated power 1420 trs/min rated rotational speed and 50

Hz, 220 V rated stator impressed voltage. The values of the motor parameters are as follows:

$R_s = 4.85\ \Omega$; $R_r = 3.805\ \Omega$; $L_s = 0.274$ H; $L_r = 0.274$ H; $L_m = 0.258$ H;

$J = 0.031\ \text{kg.m}^2$; $f = 0.00114$ Nms.

The first test concerns a no-load starting of the motor with a reference speed $\Omega_{ref} = 100\ \text{rad/s}$, then a load torque of 10 Nm is applied between 0.8 sec and 1.5 sec. The test results obtained are shown in figure 3.

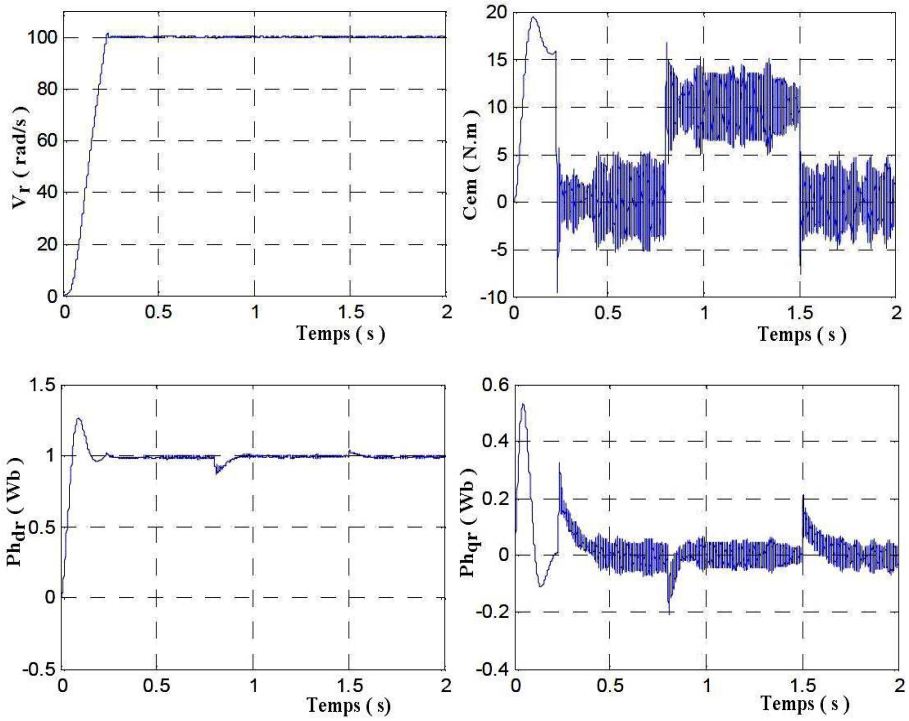

Fig. 3: Simulation results for the sliding mode control

The waveforms depicted in the above figure show that the ideal field-oriented control is established by setting the flux responses $\Phi_{qr} = 0$ Wb and $\Phi_{dr} = 1$ Wb. It can be noticed as well that during the reverse speed operation, the actual rotor speed tracks the desired speed.

The inversion of speed response causes a step change in the torque response T_{em} without any effects on the fluxes responses, which are maintained constant, due to the decoupled control introduced by the proposed hybride approach between speed and rotor flux. So, these characteristics are similar to those obtained with a D.C Machine, which is the aim of the proposed approach.

This latter has the advantage of not being based on the defluxing block as in the conventional field oriented control. Further, the decoupling between speed and flux is maintained for the whole range of speed.

One can notice the oscillations of the torque and the pulsation of the current i_{as}, due to the discontinuous characteristic of the controller causes by chattering phenomenon.

The second test concerns the robustness towards the variation of the rotor resistance R_r (90 % of nominal value), the same test as above is carried out (Fig. 4).

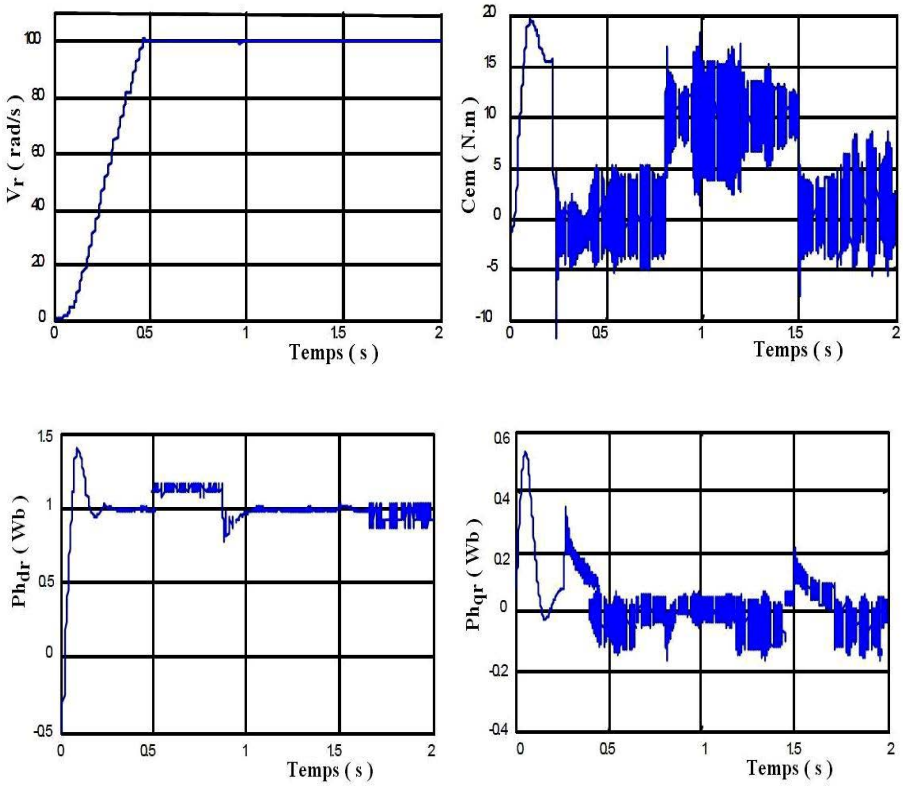

Fig. 4: Simulation results for the sliding mode control (variation of 90 % R_r)

The responses in figure 4 show that the performances of the proposed approach are not too affected by the variation of rotor resistance R_r. In fact, the waveforms are similar to those obtained in section 5.

It is clearly shown that the reference input is perfectly tracked by the speed and the introduced perturbation is immediately rejected by the control system in the steady state. These results were predictable due to the use of the sliding mode control.

6. IMPROVEMENT OF PERFORMANCES OF THE INDUCTION MOTOR BY USING ROBUST NEURAL NETWORKS

The artificial neural network make use of nonlinearity, learning, parallel processing, and generalization capabilities for application to advanced intelligent control [1, 2]. This general non-linear approximation capability of neural Networks offers great potential for non-linear control.

This study deals, in a rigorous analysis, with the introduction of two robust artificial neural network controllers (RANNCs), in the hybrid control system which illustrated in figure 2. The objective of RANNCs is to mimic the non-linear control laws given by the sliding mode controllers [4].

It is well known that there is no general guideline for choosing the appropriate network configuration for a given problem. This makes difficult the selection of the optimal network configuration, but also gives us an insight to the sensitivity of adjusting network architecture. The structure of the proposed multiplayer perceptron network is constituted by three layers of non-linear processing nodes as follows [6]:

1. Input layer = 2 neurons (units)
2. Hidden layer = 9 neurons (units)
3. Output layer = 1 neuron (unit)

The RANNCs adopted are feed-forward in the sense that each unit receives inputs only from units in the preceding layer. The input signals are then converted by the neural net according to the following equation:

$$y = f\left(\sum_{i=1}^{N} w_i x_i - b_i \right) \tag{22}$$

where $(x_1, x_2, \ldots, x_N)$ are inputs from the previous layer neurons, $(w_1, w_2, \ldots, w_N)$ are the corresponding weights, b_i is the biases of the neurons, and f is the activation function. In the RANNC, each nonlinear processing node is characterized by a tanh-sigmoidal activation function, except the one corresponding to the output neuron, which is a linear function

Concerning the training algorithm used in this work is the Levenberg-Marquardt which is based on the recent researches and proves that this algorithm permit a reduction of the number of iterations.

6.1 The training design of the robust artificial neural network speed controller (RANNC1)

The inputs to the network are considered as the errors $e_1(t)$ and $e_1(t-1)$ between the reference variable Ω_{rref} and the real value Ω, estimated respectively at time t and $(t-1)$. The output is the reference variables i_{qs1}^{*} [4].

One possible structure of teaching the robust speed regulator law to the RANNC1, is shown in figure 5. It is based on the ability of the neural network to form a nonlinear control law given by the sliding mode speed controller (SMC1).

The inputs training data, considered as the incorporated historic data, and have a significant part of the learning process. Thus, in order to learn the sliding mode speed controller law to the RANNC1, the training procedure with the Leverberg-Marquardt algorithm with the same test as in section (5) is carried out by considering 1000 examples taken between 0 sec and 0.5 sec for a reference speed $\Omega_{ref} = 100\,\text{rad/s}$.

The network converged to the fixed error of 1 % after 700 iterations. After that, a cross-validation is carried out with the same test as above, with 1500 examples data training set. This training process proves that the network has learned the nonlinear control law of the SMC1.

6.2 The training design of the rotor flux robust neural network controller (RANNC2)

By using a similar procedure as above, the rotor flux sliding mode controller (SMC_2) used in figure 5, is replaced by a robust neural network controller.

In this case, the same architecture of previous neural network (2-9-1) is adopted. The inputs to the $RANNC_2$ are chosen as the difference between the flux reference Φ_{rref} and the estimated value Φ_r considered at time t and $(t-1)$ respectively. Note that, the output is considered as the command variable i^*_{ds1}. The proposed training procedure is done by using the $RANNC_1$ as a speed controller.

The input training data are the same as those considered in section (5). So, in this case, the sum-squared error between the desired value of i^*_{ds} and the controller output i^*_{ds1} reached 1 % after 500 iterations. The training algorithm forces the estimated $i^*_{ds1}{}^*$ to follow the desired variable command i^*_{ds1}.

After that, in order to verify if the robust neural control would be capable of driving the plant in all the operating range and without instability, a period of on-line specialized learning would then be used in the following section to improve the control provided by the two neural networks controllers.

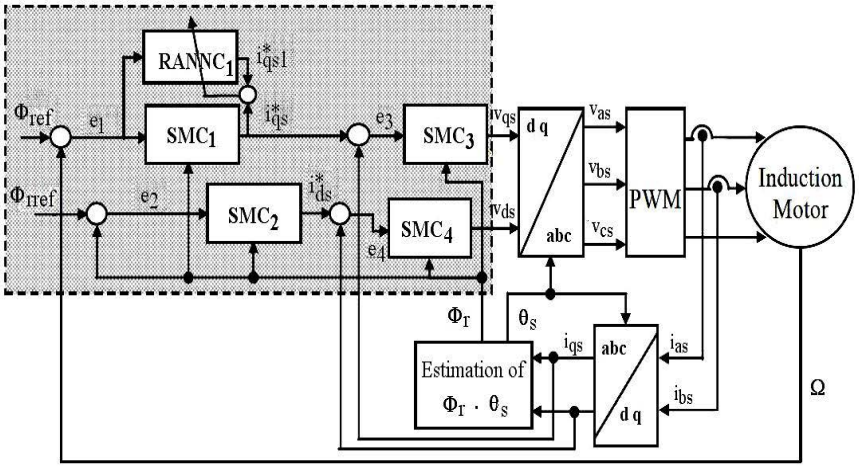

Fig. 5: Training design of $RANNC_1$

6.3 Validation of the speed regulation with robust artificial neural network controllers (RANNCs)

The same tests as in section 5 were carried out. The results obtained are given in figures 6 and 7 which correspond to the simulation test without any variation in parameters and the case with 90 % of Rr variation, respectively.

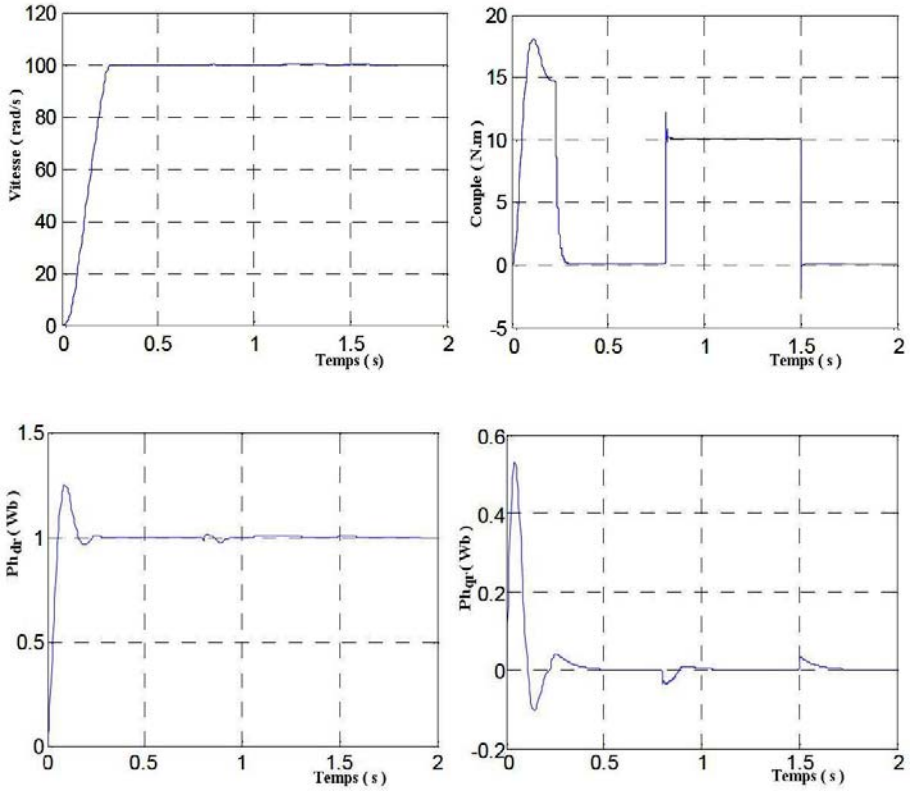

Fig. 6: Simulation results for the RANNC control

The responses obtained with the neural networks controllers are highly similar to those illustrated in figures 3 and 4. We can also notice that the decoupling of the motor variables (Flux-torque) is indeed maintained and that their responses stay regulated to their respective set commands.

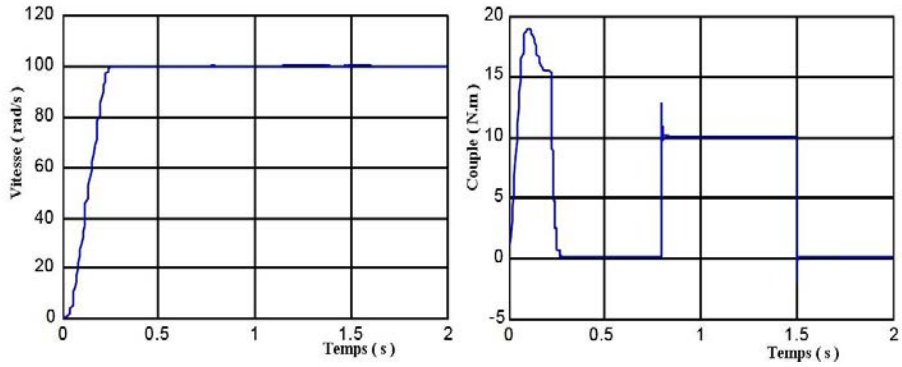

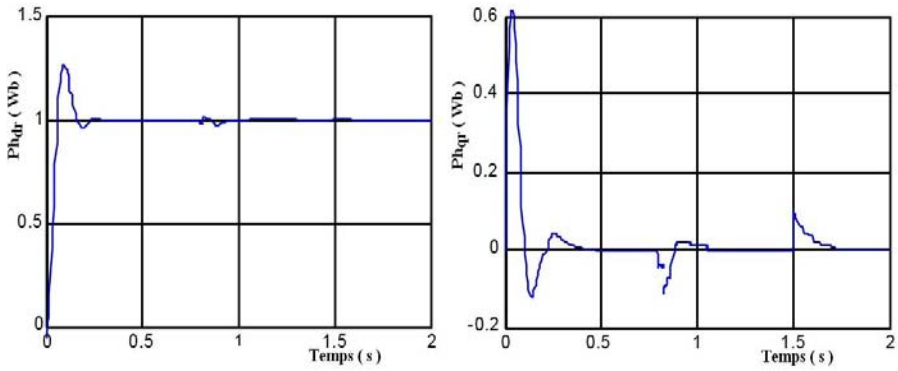

Fig. 7: Simulation results for the RANNC Control
taking into account the variation of 90 % Rr

On the other hand, these neural networks controllers permits the establishment of the condition of field-oriented control in steady state ($\Phi_{qr} = 0$) and ensure the robustness towards parameter's variations. We also could notice that the chattering is approximately inexistent here. Then, we can conclude that our objective is attempt with success.

7. CONCLUSION

The proposed approach has revealed very interesting features. In fact, as first step, the combination of the nonlinear control with the field oriented control maintains an effective decoupling between speed and flux for the whole range of speed which allows to obtain high dynamic performances for constant flux operation similar to that of DC motors.

Further, these high performances are maintained above the nominal speed for the constant power operation, which is not the case in the conventional field oriented control. The addition of the sliding mode controllers has improved the robustness towards internal parameter variations, modelling uncertainties and external disturbances.

In addition the proposed control scheme provides a good protection to the connected inverter and motor, against high stator currents since these latter are controlled. Further, compared to the conventional field-oriented control, this approach is simple to implement.

Concerning the development of the attractivity control, a smooth control function with a threshold is adopted.

Nevertheless, the magnetic of this reachability control depends closely on the upper bound of uncertainties, which include parameter variations and external disturbances. So, an adequate choice of these parameters is needed, especially in order to reduce the chattering. However, the bound is difficult to obtain in advance for motor operates.

Thus, two RANNCs are investigated in order to highlight the effectiveness and performances of the developed control scheme. The simulation results demonstrate the effectiveness of the designed control scheme.

The robustness and the tracking qualities of the proposed control system using RANNC appear clearly. The most important remark is that the chattering is significantly reduced or being inexistent.

Finally, we can conclude that the objective by the proposed approach was attempt.

NOMENCLATURE

i_{ds}^* , i_{qs}^* : Stator current $d-q$ axis references

i_{ds} , i_{qs} : Stator current $d-q$ axis components

V_{ds}^* , V_{qs}^* : Stator voltage $d-q$ axis references

V_{ds} , V_{qs} : Stator voltage $d-q$ axis components

Φ_{dr} , Φ_{qr} : Rotor flux $d-q$ axis components

R_s , R_r : Stator, rotor resistances

Φ_{rref} : Rotor flux command

L_s , L_r : Stator, rotor inductances

T_r : Rotor time constant (L_r / R_r)

L_m : Mutual inductance

p : Pairs of poles

Ω : Mechanical speed

J : Moment of inertia

T_r : Load torque

σ : Tota leakage coefficient $\sigma = \left(1 - L_m^2 / (L_r - L_s\right)$

REFERENCES

[1] D. Psalti, A. Sideris, A. Yamamura, '*Neural Controllers*', *Proceedings of 1st International Conference on Neural Networks, Vol. 4, pp. 551 – 558*, San Diego, USA, Vol. 4, pp. 551 - 558, 1987.

[2] M.O. Efe and O. Kaynak, '*A Comparative Study of Neural Network Structures in Identification of Non-Linear Systems*', Mechatronics Journal, Vol. 9, N°3, pp. 287 – 300, 1999.

[3] F. Filipeetty, G. Franceschini and C. Tassoni, '*Neural Network Aided on-Line Diagnostics of Induction Motor Rotor Faults*', IEEE Transactions on Industry Applications, Vol. 31, N°4, pp. 892 – 899, 1995.

[4] L. Barazane, '*Application des Systèmes Emergents à la Commande d'un Moteur Asynchrone*', Thèse de Doctorat d'Etat, ENP, Alger, 2003.

[5] F. Blaschke, '*The Principle of Field-Orientation as Applied to the New Transvector*', Siemens Review, Vol. 34, N°5, pp. 217 - 222, 1972.

[6] V.I. Utkin, '*Sliding Mode Control Design Principles and Application to Electric Drives*', IEEE Transactions on Industrial Electronics, Vol. 40, N°1, pp. 23 – 26, 1993.

[7] M.H. Park and K.S. Kim, '*Chattering Reduction in the Position Control of Induction Motor Using the Sliding Mode*', IEEE Transactions on Power Electronics, Vol. 6, N°3, pp. 317 – 325, 1991.